

**Tropospheric Emission Spectrometer (TES)**  
**for the Earth Observing System (EOS) CHEM Satellite.**

**I: Objectives, Requirements & Instrument Overview**

**Reinhard Beer, Thomas A. Glavich and David M. Rider**

Jet Propulsion Laboratory

California Institute of Technology

Pasadena, CA

**Abstract**

The Tropospheric Emission Spectrometer (TES) is an imaging infrared Fourier transform spectrometer scheduled to be launched into polar sun-synchronous orbit on the Earth Observing System (EOS) CHEM satellite in December 2002. We describe how the overall mission objectives flow down to the specific science and measurement requirements and how, in turn, these are implemented in the flight hardware.

Keywords: Atmospheric composition; Ozone; Remote sensing; Spectrometers and spectroscopic instrumentation; Spectroscopy, Fourier transforms

Address for correspondence:

Dr. Reinhard Beer

M/S 183-301

The Jet Propulsion Laboratory

4800 Oak Grove Drive

Pasadena, CA 91109

Tel: (818) 354-4748

FAX: (818) 393-4445

e-mail: Reinhard.Beer@jpl.nasa.gov

## Introduction

### The EOS CHEM Mission

In January 1988, NASA invited proposals for participation in a new program of polar Sun-synchronous orbiting platforms to be called the Earth Observing System (EOS). The objectives of this program have been stated in a variety of forms but most succinctly as a series of questions.<sup>(1)</sup>

- 1) What are the nature and extent of land-cover and land-use change and the consequences for sustained productivity?*
- 2) How can we enable regionally useful forecasts of precipitation and temperature on seasonal-to-interannual time frames?*
- 3) Can we learn to predict natural hazards and mitigate natural disasters?*
- 4) What are the causes and impacts of long-term climate variability and can we distinguish natural from human-induced drivers?*
- 5) How and why are concentrations and distributions of atmospheric ozone changing?*

The Tropospheric Emission Spectrometer (TES) was successfully proposed for this mission, the particular emphasis being on Question 5 but with some useful input into Questions 2, 3 & 4.

After a number of program reviews and restructurings, the spaceborne part of the program was divided into 3 parts: a largely Earth-surface orientated platform called "TERRA"; a second platform, named "AQUA", to concentrate on climate and a third one called "CHEM" to study the chemistry of the troposphere and lower stratosphere. TES was assigned to this latter platform as were three other instruments - the Microwave Limb Sounder (MLS), the High Resolution

Dynamics Limb Sounder (HiRDLS) and the Ozone Measuring Instrument (OMI). The CHEM satellite (Fig. 1) will be launched in December 2002 into a Sun-synchronous orbit with a nominal 1:45 p.m. equator crossing time. The orbit repeats exactly every 16 days (= 233 orbits) with a near-repeat every 2 days.

---

Fig. 1 here?

---

### **The Troposphere**

The *troposphere* is the region of the Earth's lower atmosphere that is dominated by convective processes. It extends from the surface, with declining temperature, up to the boundary with the stratosphere (the *tropopause*). The height of the tropopause varies with latitude and season, generally being highest in the tropics and lowest at the poles. An average thermal structure of the atmosphere is shown in Fig.2.

---

Fig. 2 here?

---

The troposphere is, in turn, often sub-divided into vertical zones. The lowest 1-2 km is termed the *boundary layer*, a region of strong horizontal and vertical mixing. Above this is the *free troposphere* where much of the important photochemistry occurs. At the top is the *upper troposphere* wherein transport to and from the stratosphere becomes important.

## **TES-Specific Objectives**

The primary objective of TES is to map the global 3-dimensional distribution of tropospheric ozone ( $O_3$ ) and the chemical species involved in its formation and destruction (so-called “precursors”). This is a very ambitious objective because a) only about 10% of the total ozone in the Earth’s atmosphere is in the troposphere - most is in the stratosphere through which, of course, any spaceborne system must observe, and b) many of the critical precursors exist only at very low concentrations (fractions of a part-per-billion by volume, ppbv). It therefore requires a very carefully designed, high performance, instrument to make the necessary measurements. In particular, such low concentrations can generally only be measured by the technique of limb sounding (a sideways view through the atmosphere), which increases the path length some 100-fold at the expense of poorer spatial resolution along the line of sight.

On the other hand, the major species such as ozone itself, water vapor, carbon monoxide and methane are readily measured by nadir viewing (with better localization but relatively limited vertical resolution), so an initial requirement on TES is that it must provide both limb and nadir sounding capability.

## **Tropospheric Ozone**

Ozone is produced in the troposphere by photochemical oxidation of carbon monoxide (CO) and hydrocarbons in the presence of nitrogen oxides (NO<sub>x</sub>) and water vapor (H<sub>2</sub>O). These ozone precursors have both natural and anthropogenic sources. The chemistry of ozone is complex and tightly coupled to the atmospheric transport of both ozone and its precursors.

Tropospheric ozone has three major environmental impacts:

- 1) *As an air pollutant.* Ozone in surface air is toxic to humans, animals and vegetation. It is the principal harmful component of smog.
- 2) *As a cleansing agent.* Photolysis of ozone in the presence of water vapor is the primary source of the hydroxyl radical (OH), which is the main oxidant in the atmosphere. Reactions with OH in the lower and middle troposphere are the principal sink for a large number of environmentally-important species including air pollutants (CO), greenhouse gases (CH<sub>4</sub>), and gases depleting the stratospheric ozone layer (HCFC's, methyl halides).
- 3) *As a greenhouse gas.* Ozone in the middle and upper troposphere is an efficient greenhouse gas. Perturbation of ozone in this region of the atmosphere results in heterogeneous radiative forcing with complicated implications for climate.

The environmental implications of tropospheric ozone are therefore very different from those of stratospheric ozone. The ozone layer in the stratosphere shields the Earth's surface from solar UV-B radiation, and thinning of this layer as a result of human activities is a matter of grave concern. Tropospheric ozone, by contrast, has increased as a consequence of human activity

(primarily because of combustion processes). Whether this increase in tropospheric ozone is beneficial (cleansing agent) or harmful (air pollutant, greenhouse gas) depends to a large extent on its altitude. It is very important, therefore, to map the global 3-dimensional distribution of tropospheric ozone and its precursors in order to improve our understanding of the factors controlling ozone in different regions of the troposphere.

### **TES Data Products**

In the EOS program, data products are divided into 2 classes: Standard Products, which are produced routinely and archived in a publically-accessible location, and Special Products, which have more of a research nature and are produced on an “on demand” and non-interference basis.

The Standard Products that TES will produce are global-scale vertical concentration profiles (0 - ~35 km) of ozone, water vapor, carbon monoxide, methane, nitric oxide, nitrogen dioxide and nitric acid (the latter 3 in the mid- and upper troposphere only) every 4 days out of 8. Essential by-products of the analysis are atmospheric temperature profiles and surface temperature and emissivity. Table I lists the Standard Products and Table II is a partial list of potential Special Products. In both cases, an indication of the necessary observation conditions is shown.

---

Table I here?

---

---

Table II here?

---

## Measurement Requirements and Approaches

### Introduction

The science requirements outlined above lead directly to a set of instrument and measurement requirements, shown in Table III. The detailed basis and justification for these requirements is far too long to reproduce here so only a brief outline follows. Further details can be made available on request<sup>(2)</sup>.

---

Table III here?

---

*Spectral Properties.* The species to be observed have their transitions widely scattered throughout the infrared, so an initial requirement is for broad spectral coverage (650 - 3050  $\text{cm}^{-1}$ ). Secondly, we want the spectral resolution to match the widths of the spectral features. Near the surface, weak Lorentz-broadened lines have a width  $\sim 0.1 \text{ cm}^{-1}$ , falling to  $\sim 0.025 \text{ cm}^{-1}$  in the upper troposphere. Note that, within a factor of about 2, these widths are independent of species and frequency, so we have chosen those values for the nadir and limb modes respectively. In turn, this requires a maximum optical path difference (OPD) of 8.45 cm in the nadir and 33.8 cm at the limb, resulting in spectral sampling distances of  $0.0592 \text{ cm}^{-1}$  and  $0.0148 \text{ cm}^{-1}$  respectively. For a number of reasons, it is preferable that zero path difference (ZPD) be in the middle of the travel so these values are bi-directional. Furthermore, we have chosen to use a constant-speed mechanism to change the OPD, resulting in scan times of 4 seconds in the nadir and 16 seconds at the limb.

*Spectrometer Type.* The foregoing requirements lead inevitably to a Fourier Transform spectrometer (FTS)<sup>(3)</sup> because: a) dispersive spectrometers do not have constant (frequency)

resolution; b) gas correlation spectrometers are limited in the species they can observe and cannot cope with Doppler shifts and c) other technologies offer only restricted spectral coverage. We have chosen the Connes'-type 4-port configuration<sup>(4)</sup> because (as discussed below) it permits us to optimize detector technologies by using 4 relatively-limited spectral regions which are further subdivided into 200 - 300  $\text{cm}^{-1}$  bands through the use of interchangeable filters for background control and data-rate reduction.

*Detector Arrays.* One of the features of an FTS is that it readily supports an imaging mode which, in turn, improves collection efficiency over the more traditional spatially-scanning systems. We have chosen to employ 1x16 linear arrays whose size in one dimension was selected to provide an individual pixel size of 2.3 km vertically at the limb and, in the other direction, 23 km parallel to the limb. Since the same arrays are also used in nadir, these number translate to 0.5 km in-track and 5 km cross-track (Fig. 3). Furthermore, since the data from an FTS are very sensitive to non-linearities, we wished to avoid using photoconductors; thus all 4 arrays are photovoltaic Mercury Cadmium Telluride (MCT).

---

Fig. 3 here?

---

*Signal-to-Noise Ratio.* As a rough rule-of-thumb, when the spectral signal-to-noise ratio falls below 30:1 it becomes very difficult to extract useful information from the data. Thus we have, somewhat arbitrarily, chosen 30:1 as our lower limit. With a 5 cm aperture and a scan time of 4 seconds (nadir) or 16 seconds (limb), we find (using a radiometric model) that at frequencies below about 2500  $\text{cm}^{-1}$  we should be able to meet or exceed this goal under most conditions. At higher frequencies, some pixel and/or scan averaging will usually be necessary at nadir (even

under sunlit conditions) and limb sounding becomes impracticable.

At the other extreme, the upper bound to signal-to-noise ratio is limited to about 600:1 by the 16-bit analog-to-digital converter (the best that can currently be obtained as a flight-qualified component).

*Pointing Accuracy.* We use TES in a “staring” mode to avoid amplitude modulations due to scene variations (which can easily become the dominant noise source in an FTS). This, in turn, puts stringent requirements on the pointing accuracy. Unfortunately, using active feedback control from the scene (especially at the limb) is impracticable, so we must control the pointing mirror by “dead reckoning” using gyro attitude signals from the spacecraft. The most difficult direction is the pitch axis (the vertical direction at the limb) where a specification of 74  $\mu\text{rad}$  peak-to-peak is necessary due to the extreme radiance gradients (up to 40% per km) observed in the upper troposphere.

*Field of Regard.* The 2-axis pointing mirror not only must stabilize the line of sight but must also permit switching the field of view a) from nadir to the (trailing) limb, b) to cold space above the limb and c) to the internal calibration sources. This has the added benefit that TES is not limited to strictly nadir viewing - we can offset the downward view by up to 45° in any direction and either stare at a location (a volcano, for example) for over 3 minutes or, along the ground track, place the footprints contiguously to make transect observations covering more than 800 km. This mode is valuable for observing phenomena such as the regional ozone episodes that invade the eastern US in the summer.

## Instrument Overview

### Optical Layout

As indicated in Table III, TES is a Connes'-type 4-port imaging infrared Fourier Transform Spectrometer. Fig. 4 shows a schematic of the optical path and Fig. 5 is a photograph of a full-scale mock-up of the complete instrument before the thermal blankets are installed.

---

Fig. 4 here?

---

Fig. 5 here?

---

Key features of TES are the use of:

- i) Back-to-back cube corner reflectors on a common translator mechanism to provide the change in optical path difference.
- ii) KBr for the beamsplitter/recombiner and the compensator. While KBr has many desirable properties such as good infrared transmittance and a low refractive index, it has numerous less-desirable ones such as low strength and resistance to deformation and is, of course, hygroscopic. While these certainly complicate handling and mounting, KBr has been used in space successfully in other instruments (e.g., ATMOS)<sup>(5)</sup>;
- iii) Only one of the two input ports for actual atmospheric measurements. The other input views an internal, grooved, cold reference target.
- iv) A diode-pumped solid-state Nd:YAG laser for interferogram sampling control. The lower voltages and power dissipation of the Nd:YAG laser compared to, for example, a HeNe laser make it, in our view, a better choice despite the need for temperature control of the laser head;
- v) Cassegrain telescopes for condensing and collimating wherever possible in order to minimize

the number of transmissive elements in the system;.

vi) A passive space-viewing radiator (see below) to maintain the interferometer and most of the associated optics at 180 K. This reduces the thermal background noise and improves contrast between the scene and the instrument background;

vii) A 2-axis gimballed pointing mirror operating at ambient temperature to permit observation over the full field-of-regard (a 45° cone about nadir plus the trailing limb). Pointing is performed by “dead reckoning”: the gimbal axes have 21-bit shaft encoders attached and, using these and spacecraft ephemeris and attitude information, the on-board computer calculates the necessary pointing angles.

viii) Two independent focal plane assemblies maintained at 65 K with active pulse-tube coolers. The assemblies accept the dual outputs of the interferometer (labeled “1” & “2”), which are further split by dichroics into “A” and “B” channels, whence the designations in Table III. Thus there are 4 independent focal planes, each an array of 1 x 16 elements, and optically conjugated so that equivalent pixels in each focal plane see the same target. Each focal plane is photovoltaic MCT optimized for a different spectral range (see Table III). In addition, each has an independent filter wheel in which the filters are typically 200 - 300 cm<sup>-1</sup> wide (Table IV). This not only reduces instrument background control but permits sampling of the interferograms in an upper alias<sup>(3)</sup> (the sampling interval is between 8 and 11 laser fringes per sample) with a consequent reduction in data rate and volume (i.e., provides a form of lossless data compression).

---

Table IV here?

---

## **Signal Chains**

Each of the 16 pixels in each array has an independent signal chain (i.e., 64 in all). The implementation uses Application-Specific Integrated Circuits (ASIC) with 4 levels of switchable gain and switchable electronic bandpass filters (designed to match the optical bandpasses) for noise control. Output is provided by 16-bit analog-to-digital converters triggered by the Nd:YAG laser sub-system. The digital outputs are multiplexed into a single packetized serial bit stream and transmitted to the spacecraft *via* a TAXI interface. The output science data rate averages 4.5 Mbps.

## **Thermal and Mechanical**

The instrument is contained in a box-shaped panel-and-web structure, largely of graphite-cyanate ester composites. The dimensions are 1.0 x 1.3 x 1.4 m. The nadir-viewing face serves as a radiator to reject heat from the electronics. Two radiating surfaces are mounted on the space viewing side of the instrument: one serves to cool a thermal shield surrounding the interferometer to 230 K while the other cools the interferometer to 180 K to minimize instrument self emission. A deployable earth shade protects these two radiating surfaces from earthshine.

Many of the heat-generating electronic subassemblies are mounted on the spacecraft side of the instrument for structural integrity, far from the nadir radiator. Propylene loop heat pipes<sup>(6,7)</sup>, a technology only recently available, are used to transport heat from these electronic assemblies to the nadir radiator. The advantages of loop heat pipes over more conventional heat pipes are that their efficiency is largely independent of orientation or gravity and they can be turned on and off

at will. The ability to turn the loop heat pipes off is particularly important for instrument decontamination where it is imperative that heat losses from the instrument are minimized to conserve decontamination power.

The interferometer is built around a separate structure called the optics bench that is mounted on the interior of the main structure. The optics bench is also fabricated from graphite-cyanate ester composites, which are designed for a near-zero coefficient of thermal expansion along critical directions. The optics bench temperature is controlled with small heaters to minimize mechanical distortions due to changing thermal gradients.

### **In-Flight Calibration**

An emission-mode sensor such as TES is critically dependent on its radiometric calibration if valid retrievals are to be made from its spectra. Accordingly, TES has an internal full-aperture cavity black body source (identical to that used on the MOPITT instrument on the TERRA spacecraft) to which the pointing mirror can be directed. The temperature of this black body is adjustable between ambient ( $\sim 290$  K) and 340 K. Most routine calibrations are performed at 340 K for the hot point and cold space for the baseline (offset). Although PV detectors are much less susceptible to non-linearity than PC detectors, the potential for non-linearity elsewhere in the signal chain always exists so, from time-to-time, the internal source will be varied in temperature over its entire range so the effect (if any) can be monitored.

Most standard calibrations will be obtained at  $0.0592\text{ cm}^{-1}$  spectral sampling distance (SSD) and

FFT-interpolated for the limb scans at  $0.0148 \text{ cm}^{-1}$  SSD. This presupposes that there are no sources of sharp-line spectral features internal to TES. Occasionally, therefore, we will acquire calibration data at the higher resolution to check this hypothesis.

TES also has an on-board spatial calibrator (an illuminated slit) that the pointing mirror will sweep over the detector arrays to check the co-alignment of the arrays.

## **Contamination**

TES is a cryogenic instrument and, as such, is very susceptible to contamination from outgassing not only internally but also from the rest of the spacecraft. Most vulnerable, of course, are the focal planes (the coldest points in the system). We will monitor this through the calibration signals - when these fall by 5%, decontamination heaters will be turned on to raise the entire instrument to about 10 C in order to drive off any condensates (primarily expected to be water vapor, carbon dioxide and residual hydrocarbons).

## **Operational Modes**

### **Introduction**

As indicated earlier, TES inherently operates in a step-and-stare mode when downlooking. At the limb the instrument points to a constant tangent height. The footprint is therefore smeared along the line of sight by about 110 km during a 16 second limb scan (comparable to the effective size of the footprint itself). Thus horizontal inhomogeneity in the atmosphere becomes an issue that must be dealt with in data processing (usually through a simplified form of tomography).

Furthermore, the long path through the limb makes cloud interference almost inevitable; rarely does a limb view penetrate to the boundary layer. Nevertheless, the benefits of limb viewing for trace gas analysis in the mid and upper troposphere are so great as to outweigh any disadvantages.

### **Global Surveys**

The routine operating mode for TES is to make continuous sets of nadir and limb observations (plus calibrations) on a 4-day-on, 4-day-off cycle (58 orbits each). During the “off” days, extensive calibrations and Special Product observations are made (see below). The main argument for such discontinuous sequencing is the sheer volume of data generated in 4 days (about 650 Gb). This stresses not only the data analysis process but, more importantly, the ability of the scientific community to assimilate the information.

An overview of the acquisition process is shown in the upper part of Fig.6. The lower part shows how this is broken up into 81.2 second sequences of calibration, nadir and limb observations. The timing is based on the need for the sampling density to be commensurate with the roughly 5° latitude grid of current chemical/dynamical atmospheric models. Furthermore, acquisition is triggered by the crossing of the southernmost point in the orbit (the southern apex). Thus observations are made at the same latitudes on every orbit and, every 16 days, identical locations sampled (Fig. 7).

---

Fig. 6 here?

---

Fig. 7 here?

---

### **Intensive Campaigns**

Intensive Campaigns fall under the “Special Product” rubric and are necessarily conducted in-track. There are two types presently envisaged: downlooking transects and continuous limb observations. Transects involve pointing forwards  $45^\circ$  and staring for one or more 4 second scans. The footprint is then stepped backwards so that the new footprint is contiguous to the previous one (Fig. 8). Of course, the spacecraft is moving forward during this time at about 7 km/s so eventually the transect passes through nadir and is terminated when the nadir angle is  $45^\circ$  backwards. The  $45^\circ$  limit is somewhat arbitrary but is roughly the condition beyond which line-of-sight inhomogeneity and refraction would complicate the analysis. Furthermore, the footprint stretches as one goes off-nadir with a consequent loss of spatial resolution. Transects can be up to 885 km long and will typically be used to study regional ozone episodes such as occur over the Eastern US in summer. Limb campaigns are unlimited in length and will usually be used to investigate upper troposphere impacts of large volcanos (exemplified by the Mt. Pinatubo eruption in 1991) and tropical biomass burning in September/October. Similar campaigns will be undertaken for intercomparisons with the other CHEM instruments and in validation programs.

---

Fig. 8 here?

---

## Special Events

Special Events use the ability of TES to point at specific locations for a few minutes on any given orbit. Notable among these targets are gas-emitting volcanos (e.g., Kilauea in Hawaii) whose gas admixtures are believed to be eruption predictors. Since TES can point anywhere within  $45^\circ$  of nadir (cross-track and in-track) almost everywhere on Earth can be reached some time during a 16 day interval.

## Data Analysis

TES data processing falls naturally into 4 groups (the “Level” terminology is NASA’s):

- 1) *At Level 1A*, the raw data from the spacecraft are decommutated and the interferograms reconstructed. File headers also contain important ancillary data such as time, date, spacecraft and target location, and instrument pointing angle.
- 2) *At Level 1B*, the interferograms are phase-corrected and converted to spectra, radiometrically-calibrated and resampled onto a common frequency grid. Certain data quality flags are added to the header at this juncture and the results passed to Level 2<sup>(8)</sup>.
- 3) *At Level 2*, vertical concentration profiles of the selected species are retrieved from the spectra<sup>(9)</sup>.

Briefly, all modern retrieval algorithms are somewhat alike: based on an initial estimate of the physical/chemical state of the atmosphere at the time and location of the observation (the so-called *first guess*), the appropriate version of the Equation of Radiative Transfer is solved to provide an estimate of the expected spectral radiance as seen by the instrument. This *forward*

*model* is compared to the observed spectral radiance and the parameters of the atmospheric state adjusted (using specified rules) to bring the forward model into closer agreement with the observation. The process is iterated until, by other specified rules, convergence is achieved. The resulting *state vector* of atmospheric parameters is the desired result. Most algorithms also provide an objective estimate of the accuracy of the retrieval.

4) *At Level 3*, the profiles are resampled onto appropriate surfaces (usually pressure) to provide a series of maps (one set for each species). This, we believe, will be the most commonly-accessed TES browse product although serious users will then most likely request the Level 2 profiles themselves. Note that it is EOS data policy that all products are in the public domain and available from the archives at the marginal cost of reproduction. TES data will be archived and available from at the NASA Langley Research Center Distributed Active Archive Center (DAAC) in Hampton, VA.

## **Instrument Status**

As of this writing, prototype hardware exists for all major sub-systems and much has been subjected to environmental testing (vibration, thermal-vacuum, etc.). However, for reasons of cost and schedule, no actual complete engineering model will be built. Instead, once the individual sub-system designs have been validated, we shall proceed directly to construction of the actual flight instrument (in a so-called “protoflight” mode). It is the protoflight hardware that will be fully tested and calibrated and, for the first time, generate actual interferograms. We eagerly await this event, due to occur in 2001.

## Conclusions

Although uncommon in this type of paper, we have felt it to be important that the reader be able to follow the reasons why specific instrument parameters and characteristics were chosen, flowing from the overall mission requirements down to the specific hardware implementation. In many cases, there were equally good or bad alternatives but over-riding requirements for any space experiment are cost and schedule. Reliability through redundancy is also preferred but cost considerations have dictated that TES be largely a single-string instrument with little or no duplication of parts.

In a subsequent paper we shall discuss the measured characteristics of TES as compared to the pre-flight performance models on which much of the design is based. However, we have high confidence that the goals will be met because TES shares many of the characteristics of an airborne precursor called the Airborne Emission Spectrometer (AES). AES has flown many times on a variety of aircraft (a severe environment for any instrument) with good success<sup>(10)</sup> and has proven to be an invaluable test-bed both for hardware and for data analysis.

## **Acknowledgments**

We should be remiss were we not to express our sincere thanks to the many individuals who have contributed to this program. The full list would run to well over 100 names but we do especially wish to thank Robert J. McNeal of NASA HQ for his long-standing support, Daniel Jacob and Jennifer Logan of Harvard University for keeping us focused on our primary objective, Tony Clough of AER Inc. and Clive Rodgers of Oxford University for their keen analytical insights, and Edward Miller and Helen Worden of JPL without whom this instrument could never be built.

The research reported in this paper was conducted by the Jet Propulsion Laboratory, California Institute of Technology, under a contract with the National Aeronautics and Space Administration.

## References

1. *Earth Science Strategic Enterprise Plan 1998-2002*, NASA HQ, Washington D.C.  
October 1998 (<http://www.earth.nasa.gov/visions/stratplan/index.html>)
2. *Tropospheric Emission Spectrometer Scientific Objectives & Approach, Goals & Requirements, Version 6.0*. JPL D-11294, April 1999.
3. Beer, R. *Remote Sensing by Fourier Transform Spectrometry*. Wiley & Sons, NY (1992)
4. Connes, J. and P. Connes, Near-infrared planetary spectra by Fourier spectroscopy. I: Instruments and results, *J. Opt. Soc. Am.*, **56**, 896-910 (1966)
5. Farmer, C.B. "High resolution infrared spectroscopy of the Sun and the Earth's atmosphere from space", *Mikrochim. Acta (Wien)*, **III**, 189-214 (1987)
6. Wolf, D.A., D.M. Ernst, and A.L. Phillips, "Loop Heat Pipes - Their Performance and Potential," 24<sup>th</sup> International Conference on Environmental Systems, Friedrichshafen, Germany, June 20-23, 1994 (SAE Technical Paper Series 941575).

7. Nikitkin, M., B. Cullimore. and J. Baumann, "CPL and LHP Technologies: What are the Differences, What are the Similarities?," 9<sup>th</sup> Annual Spacecraft Thermal Control Technology Workshop, (Sec 3.5), Aerospace Corporation, Los Angeles, CA, March 4-6, 1998.
8. Level 1B Algorithm Theoretical Basis Document JPL D-16479, Jan 1999  
(<http://www.eospso.gsfc.nasa.gov/pub/jcloss> )
9. Level 2 Algorithm Theoretical Basis Document JPL D-16474, Jan 1999  
(<http://www.eospso.gsfc.nasa.gov/pub/jcloss> )
10. Worden, H.M., R. Beer and C.P. Rinsland, Airborne infrared spectroscopy of 1994 western wildfires. *J. Geophys. Res.* **102**, 1287-1299 (1997)

## Figure Captions

Fig. 1: CAD view of the Earth Observing System CHEM Platform on orbit. The Tropospheric Emission Spectrometer (TES) is the instrument slightly to the right of center. The keyhole-shaped entrance aperture permits both downward and limb views to be obtained (indicated by “rays” emanating from the aperture).

Fig. 2: The 1976 US Standard Atmosphere Temperature Profile showing the conventional names of the divisions of the vertical structure.

Fig. 3: TES detectors projected to the Nadir and Limb. Although shown as discrete elements, the pixels are, in fact, continuous but defined by an array of contacts underneath.

Fig. 4: TES Optical Schematic (Earth upwards in this view). Light enters at the upper left. Note the three different temperature zones and the labeling of the four detector arrays.

Fig. 5: Side view of a full-size mockup of the TES instrument before thermal blanketing (Earth towards the bottom of the page). The dark structure is the graphite-composite instrument housing and the white extension to the right is a deployable cover to shade the 180K radiator from Earthshine.

Fig. 6: Phasing of nadir and limb sequences. "SP" indicates a 4 second spaceview calibration (about 300 km altitude above the surface), "BB" a 4 second view of the internal 340K blackbody, "N1" and "N2" are two 4 second atmosphere/surface scans of the same location near nadir and "L1", "L2" & "L3" are three 16 second scans of the atmosphere at the trailing limb.

Fig. 7: Coverage during a 4-day Global Survey. The CHEM platform will be in a 705 km Sun-synchronous polar orbit with an exact 16-day repeat cycle. However, as the figure shows, there is also a near-repeat every 2 days.

Fig. 8: Schematic of the TES Transect Mode. Beginning by pointing  $45^\circ$  forward (along-track), successive footprints are laid end-to-end over a distance of as much as 885 km. The transect ends at a nadir angle of  $-45^\circ$ . Note that the along-track expansion of the footprint ("keystoning") is exaggerated for clarity.

**Table I: TES Standard Products & Required Sensitivity**

Product Name	Product Source		Required Sensitivity*
	Nadir	Limb	
Level 1A Interferograms	✓	✓	
Level 1B Spectral Radiances	✓	✓	
Atmospheric Temperature Profile	✓	✓	0.5 K
Surface Skin Temperature	✓		0.5 K
Land Surface Emissivity <sup>†</sup>	✓		0.01
Ozone (O <sub>3</sub> ) VMR Profile	✓	✓	1 - 20 ppbv
Water Vapor (H <sub>2</sub> O) VMR Profile	✓	✓	1 - 200 ppmv
Carbon Monoxide (CO) VMR Profile	✓	✓	3 - 6 ppbv
Methane (CH <sub>4</sub> ) VMR Profile	✓	✓	14 ppbv
Nitric Oxide (NO) VMR Profile		✓	40 - 80 pptv
Nitrogen Dioxide (NO <sub>2</sub> ) VMR Profile		✓	15 - 25 pptv
Nitric Acid (HNO <sub>3</sub> ) VMR Profile		✓	1 - 10 pptv
Nitrous Oxide (N <sub>2</sub> O) VMR profile	✓	✓	Control <sup>‡</sup>

\* Sensitivity range maps to expected concentration range (higher concentration → higher uncertainty) . Some species (notably NO<sub>x</sub>) will require some signal averaging to meet requirements.

<sup>†</sup> Water (and, probably, snow & ice) emissivities are known and are therefore *input*, not output parameters

<sup>‡</sup> Tropospheric concentration known

**Table II: Potential Special (Research) Products**

Chemical Group	Common Name	Formula	Product Source	
			Nadir	Limb
<b>H<sub>x</sub>O<sub>y</sub></b>	Hydrogen Peroxide	H <sub>2</sub> O <sub>2</sub>		✓
	Monodeuterated Water Vapor	HDO	✓	✓
<b>C-compounds</b>	Ethane	C <sub>2</sub> H <sub>6</sub>		✓
	Acetylene	C <sub>2</sub> H <sub>2</sub>		✓
	Formic Acid	HCOOH	✓	✓
	Methyl Alcohol	CH <sub>3</sub> OH	✓	✓
	Peroxyacetyl Nitrate	CH <sub>3</sub> C(O)OONO <sub>2</sub>		✓
	Acetone	CH <sub>3</sub> C(O)CH <sub>3</sub>		✓
	Ethylene	C <sub>2</sub> H <sub>4</sub>		✓
<b>N-compounds</b>	Peroxynitric Acid	HO <sub>2</sub> NO <sub>2</sub>		✓
	Ammonia	NH <sub>3</sub>	✓*	✓
	Hydrogen Cyanide	HCN		✓
	Dinitrogen Pentoxide	N <sub>2</sub> O <sub>5</sub>		✓
<b>Halogen compounds</b>	Hydrogen Chloride	HCl	✓*	
	Chlorine Nitrate	ClONO <sub>2</sub>		✓
	Carbon Tetrachloride	CCl <sub>4</sub>		✓
	CFC-11	CCl <sub>3</sub> F	✓	✓
	CFC-12	CCl <sub>2</sub> F <sub>2</sub>	✓	✓
	HCFC-21	CHCl <sub>2</sub> F		✓
	HCFC-22	CHClF <sub>2</sub>		✓
<b>S-compounds</b>	Sulfur Dioxide	SO <sub>2</sub>	✓	✓
	Carbonyl Sulfide	OCS	✓	✓
	Hydrogen Sulfide	H <sub>2</sub> S	✓*	✓
	Sulfur Hexafluoride	SF <sub>6</sub>		✓

\* Volcanic/industrial/biomass burning plume column densities only

**Table III: TES Requirements & Specifications**

Requirement	Value or Type	Comments
Spectrometer Type	Connes'-type 4-port Fourier Transform Spectrometer	Both limb & nadir viewing capability essential
Spectral Sampling Distance	Interchangeably 0.0592 cm <sup>-1</sup> downlooking or 0.0148 cm <sup>-1</sup> at the limb	Unapodized
Optical Path Difference	Interchangeably ±8.45 cm downlooking or ±33.8 cm at the limb	Double-sided interferograms
Overall Spectral Coverage	650 - 3050 cm <sup>-1</sup> (3.2 - 15.4 μm)	Continuous, but with multiple sub-ranges typically 200 - 300 cm <sup>-1</sup> wide (Table IV)
Individual Detector Array Spectral Coverage	1A: 1900 - 3050 cm <sup>-1</sup> 1B: 820 - 1150 cm <sup>-1</sup> 2A: 1100 - 1950 cm <sup>-1</sup> 2B: 650 - 900 cm <sup>-1</sup>	All MCT PV @ 65K. For the labeling convention, see Fig. 3.
Detector Array Configuration	1 x 16	All 4 arrays optically-conjugated
Aperture	5 cm	Unit magnification system
System Étendue (per pixel)	9.45 x 10 <sup>-5</sup> cm <sup>2</sup> .sr	Not allowing for a small central obscuration from the cassegrain secondaries
Modulation Index	> 0.7; 650 - 3050 cm <sup>-1</sup>	> 0.5 at 1.06 μm (control laser)
Spectral Accuracy	±0.00025 cm <sup>-1</sup>	After correction for finite field-of-view, off-axis effects, Doppler shifts, etc.
Channeling	<10% peak-to-peak; <1% after calibration	All planar transmissive elements wedged
Spatial Resolution	0.5 x 5 km nadir; 2.3 x 23 km limb	See Fig. 4
Spatial Coverage	5.3 x 8.5 km nadir; 37 x 23 km limb	See Fig. 4

**Table III (cont): TES Requirements & Specifications**

Requirement	Value or Type	Comments
Pointing Accuracy	75 $\mu$ rad pitch 750 $\mu$ rad yaw 1100 $\mu$ rad roll	Peak-to-peak values
Field of Regard	45° cone about nadir; plus trailing limb	Also views internal calibration sources
Scan (Integration) Time	4 sec nadir & calibration; 16 sec limb	Constant-speed-scan, 4.2 cm/sec (OPD rate)
Maximum Stare Time, nadir	208 seconds	40 downlooking scans
Transect Coverage	885 km max	See Fig. 5
Interferogram Dynamic Range	$\leq 16$ bits	Plus 4 switchable gain steps
Radiometric Accuracy	$\leq 1\text{K } 650 - 2500 \text{ cm}^{-1}$ ; $\leq 2\text{K } 2500 - 3050 \text{ cm}^{-1}$	Internal, adjustable, hot black body + cold space
Pixel-to-Pixel Cross Talk	$<10\%$	Includes diffraction, aberrations, carrier diffusion, etc.
Spectral Signal-to- Noise Ratio	Up to 600:1. 30:1 minimum requirement	Depends on spectral region & target. General goal is to be source photon shot noise limited
Lifetime	5 years on orbit	plus 2 years before launch
Size	1.0 x 1.3 x 1.4 m	Earth shade stowed
Mass	385 kg	Allocation
Power, Average	334 W	Allocation
Power, Peak	361 W	Allocation
Data Rate, Average	4.5 Mbps	Science only
Data Rate, Peak	6.2 Mbps	Allocation

**Table IV: FILTER BANDS & SPECIES COVERAGE**

Filter ID	Filter Half-Power Points, cm <sup>-1</sup>		Temperatures		Major Species
Array 2B (650 - 900 cm <sup>-1</sup> )					
2B1	650	900	T <sub>a</sub>		CO <sub>2</sub> , HNO <sub>3</sub> , CFC11, NO <sub>2</sub>
Array 1B (820 - 1150 cm <sup>-1</sup> )					
1B1	820	1050	T <sub>b</sub>		HNO <sub>3</sub> , NH <sub>3</sub> , CFC11, CFC12, O <sub>3</sub>
1B2	950	1150	T <sub>b</sub>		O <sub>3</sub> , NH <sub>3</sub> , CFC11, CFC12, N <sub>2</sub> O
Array 2A (1100 - 1950 cm <sup>-1</sup> )					
2A1	1100	1325	T <sub>b</sub>		O <sub>3</sub> , N <sub>2</sub> O, HNO <sub>3</sub> , CFC12, SO <sub>2</sub> , CH <sub>4</sub>
2A2	1300	1550			O <sub>3</sub> , HNO <sub>3</sub> , CH <sub>4</sub>
2A3	1500	1750			H <sub>2</sub> O, NO <sub>2</sub>
2A4	1700	1950			H <sub>2</sub> O, NO
Array 1A (1900 - 3050 cm <sup>-1</sup> )					
1A1	1900	2250	T <sub>a</sub>	T <sub>b</sub>	O <sub>3</sub> , CO, N <sub>2</sub> O, NO, OCS
1A2	2200	2450			CO <sub>2</sub> , N <sub>2</sub>
1A3	2425	2650		T <sub>b</sub>	N <sub>2</sub> O
1A4	2600	2850		T <sub>b</sub>	HDO
1A5	2800	3050		T <sub>b</sub>	CH <sub>4</sub> , HCl, O <sub>3</sub>

**Notes:**  $T_a$  = Atmospheric Temperature Profile;  $T_b$  = Surface Temperature & Emissivity

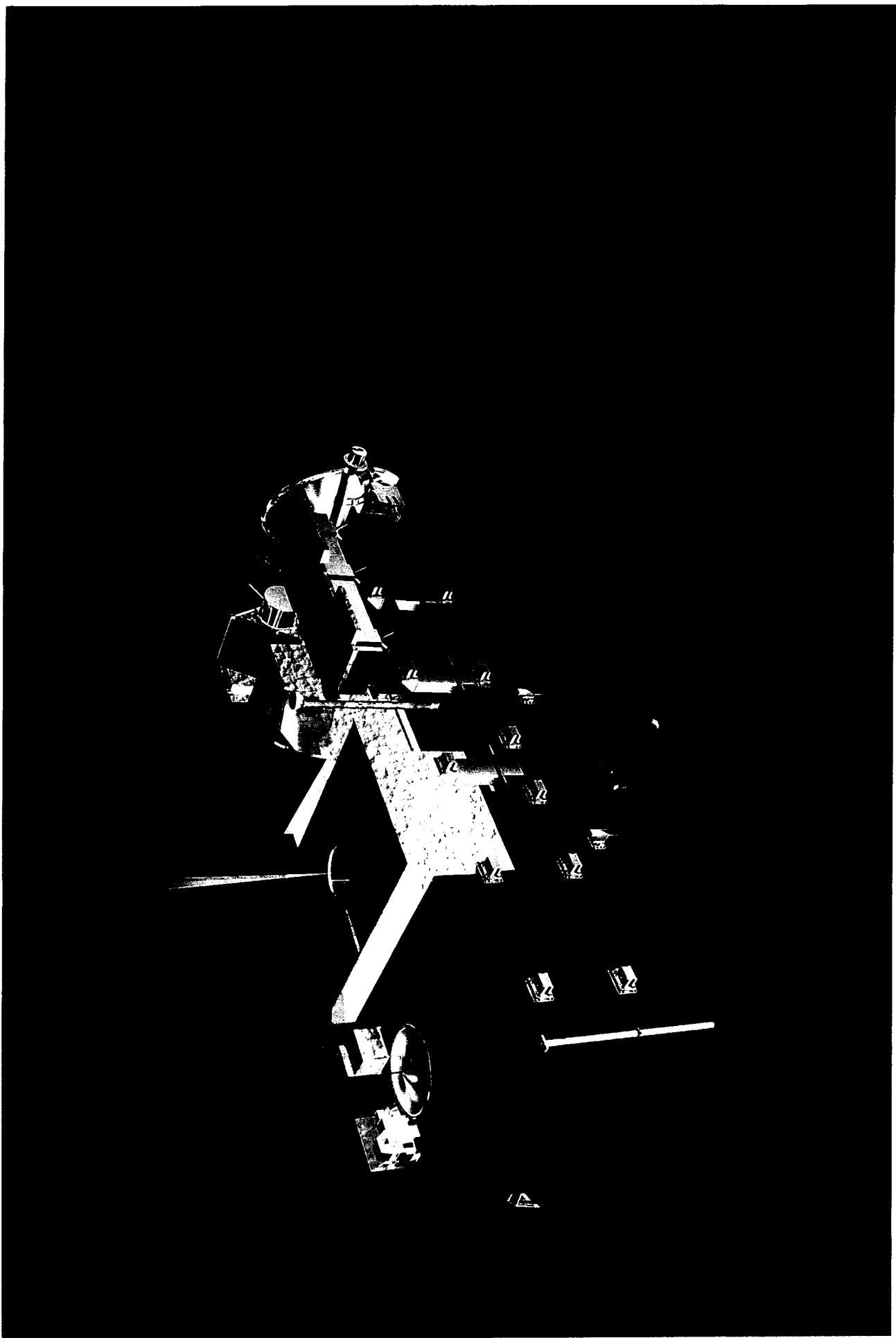


Fig 1

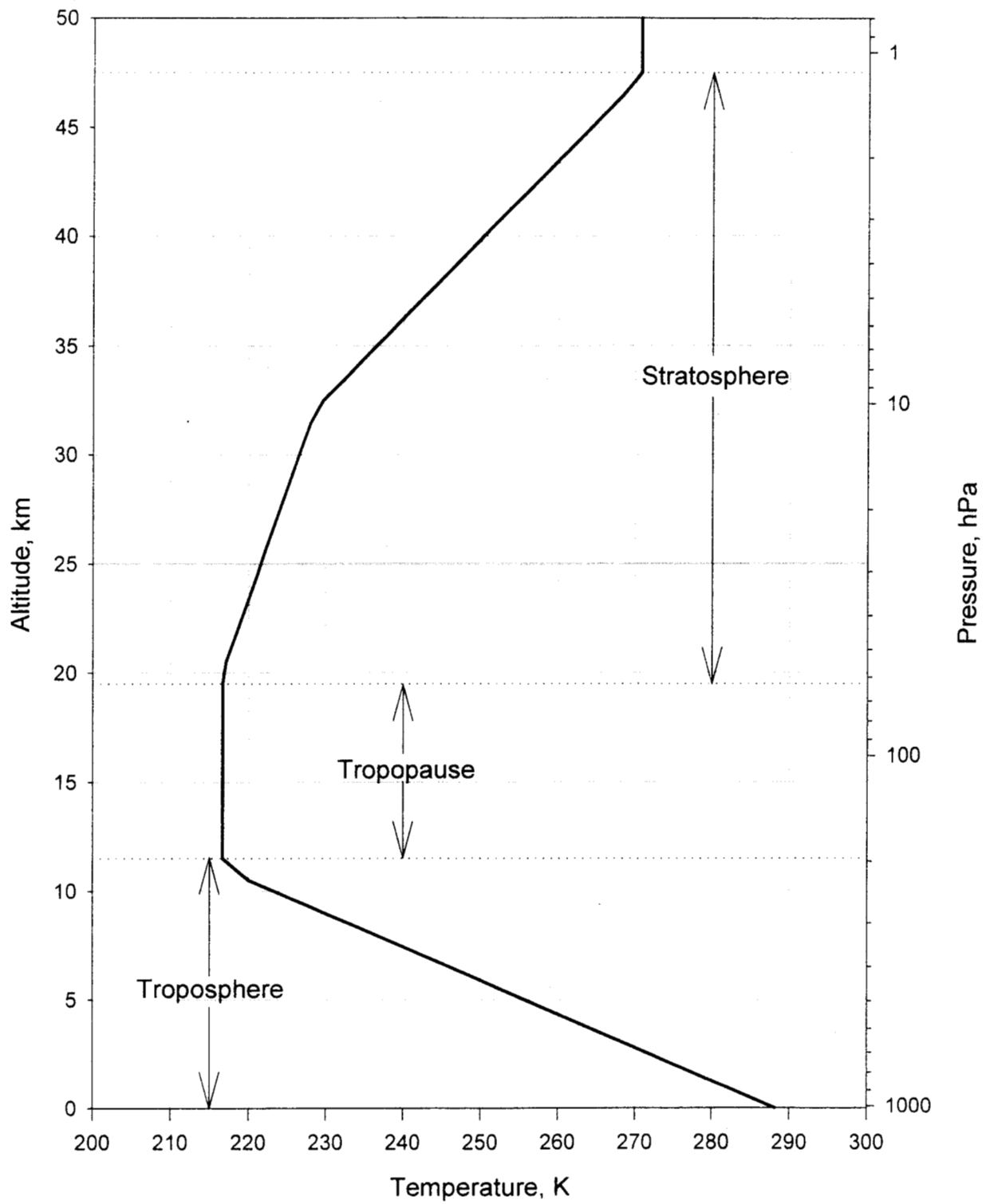
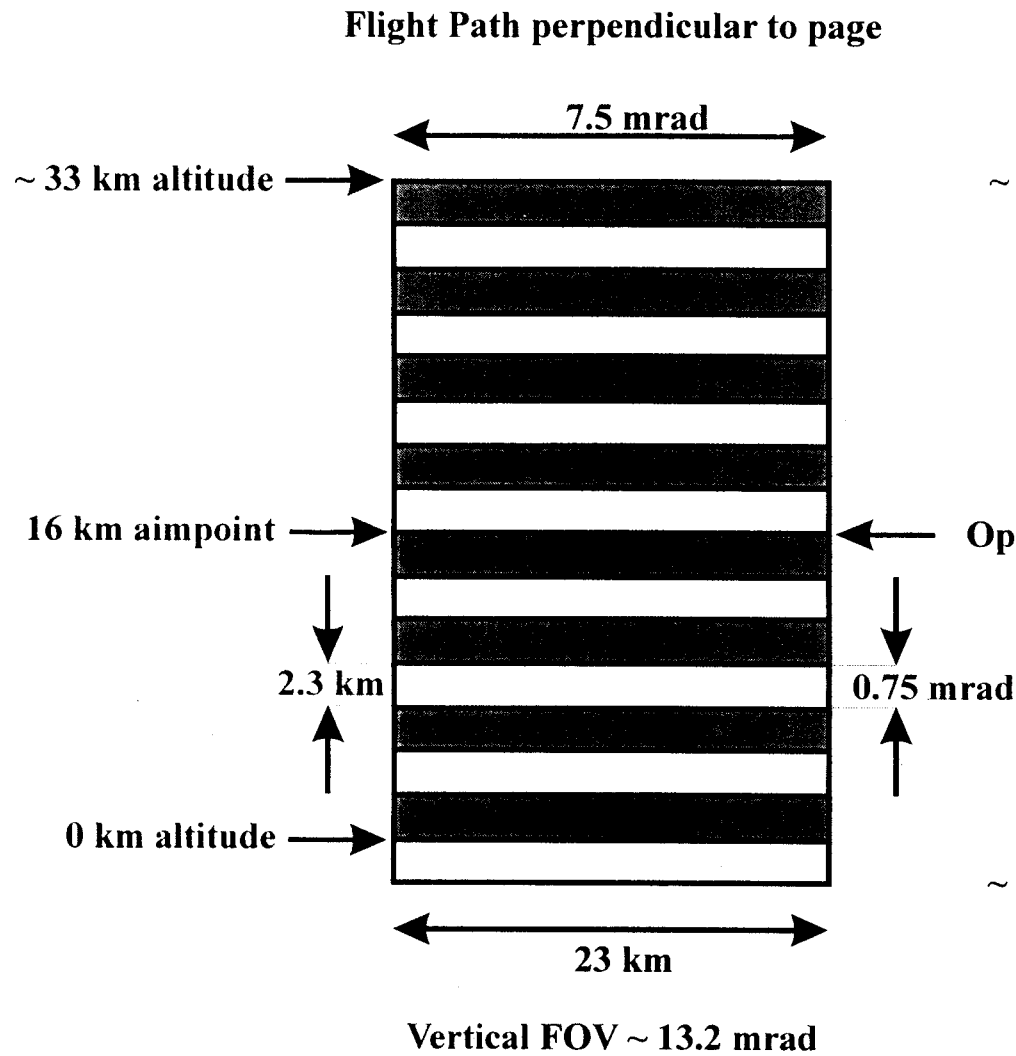
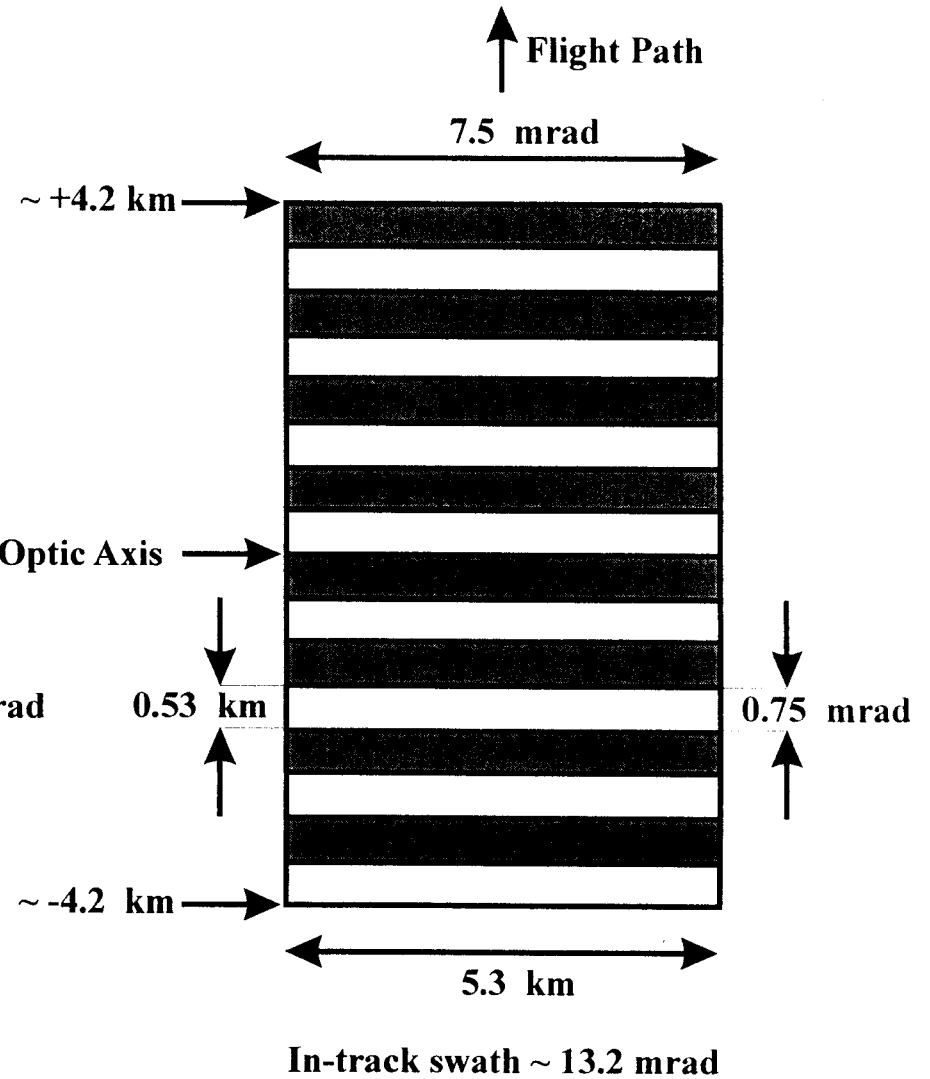


Fig. 2

## LIMB PROJECTION



## NADIR PROJECTION



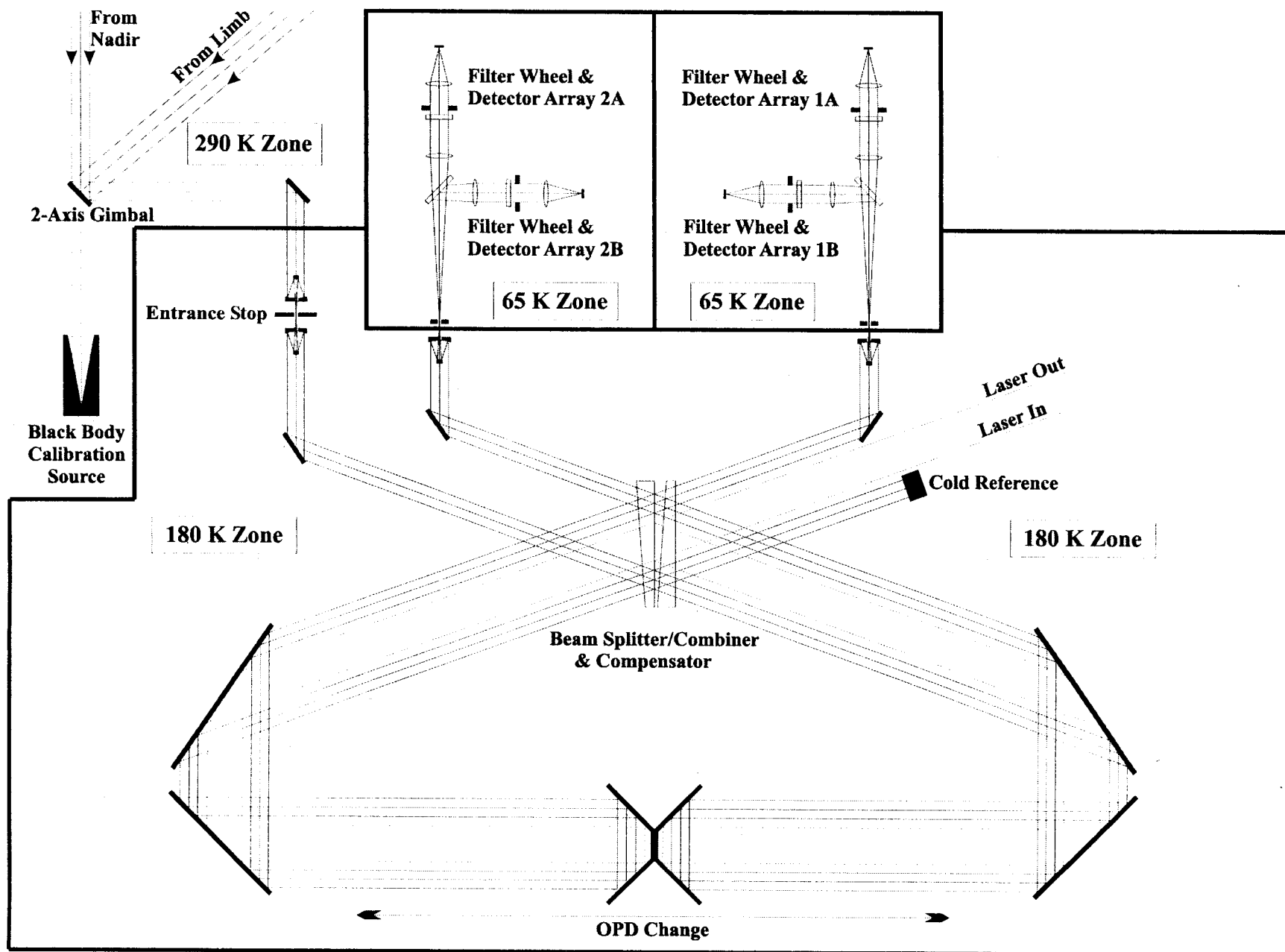


Fig. 4

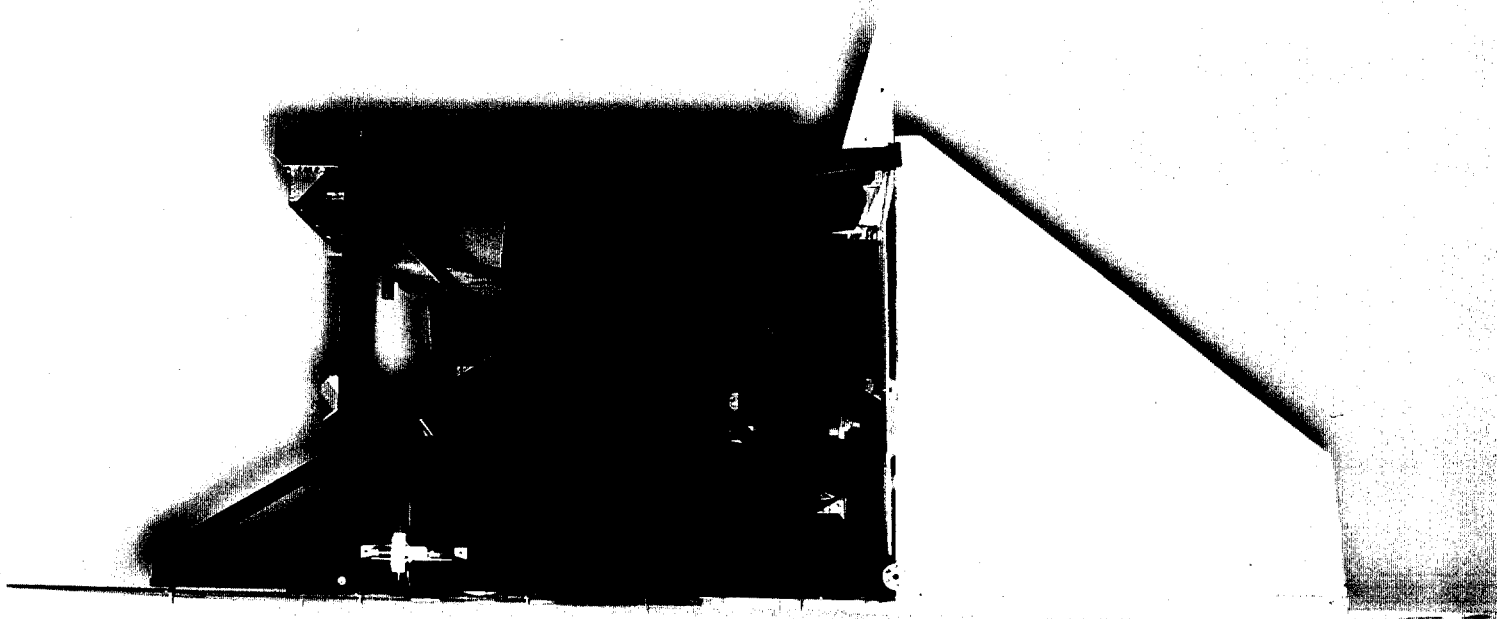
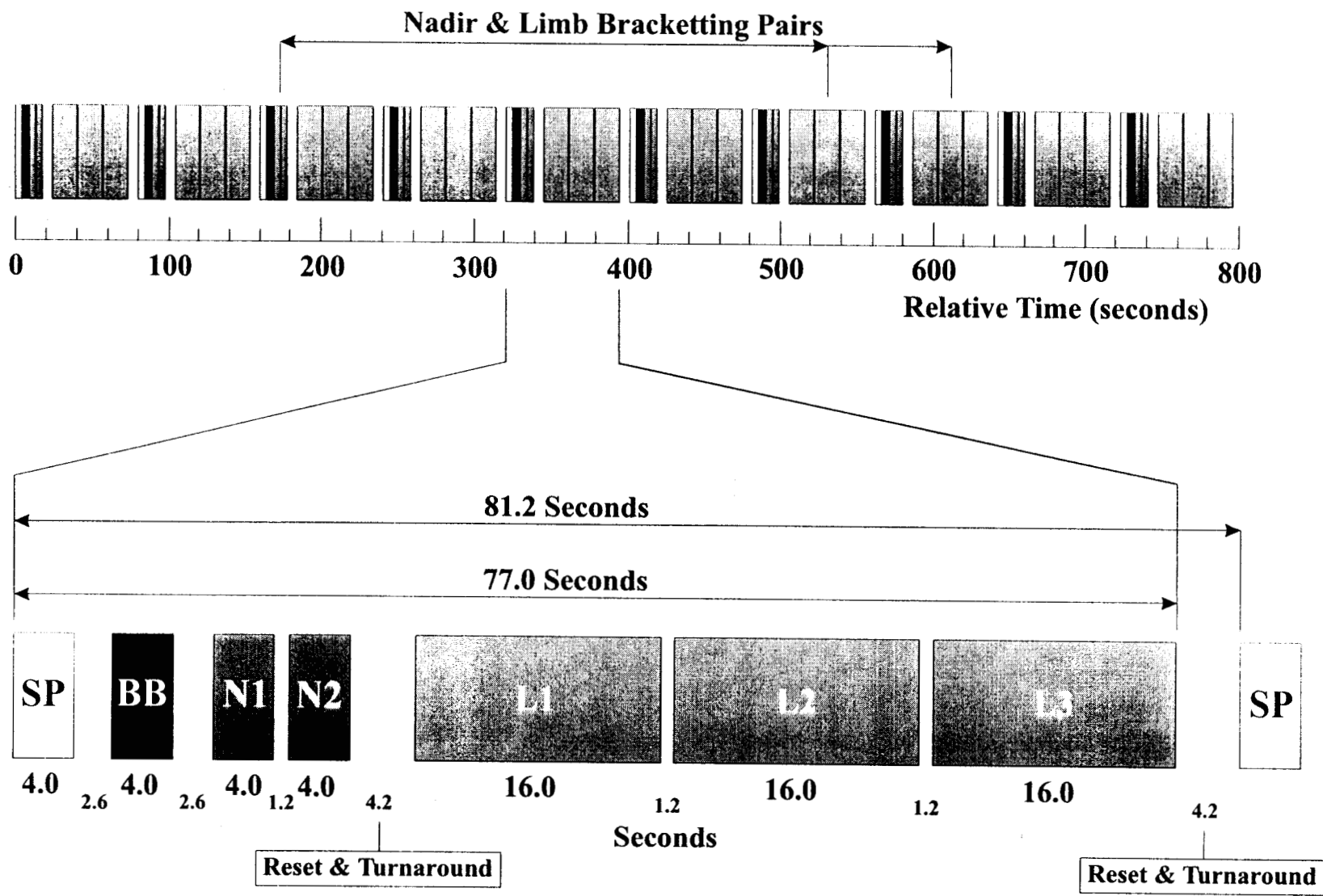
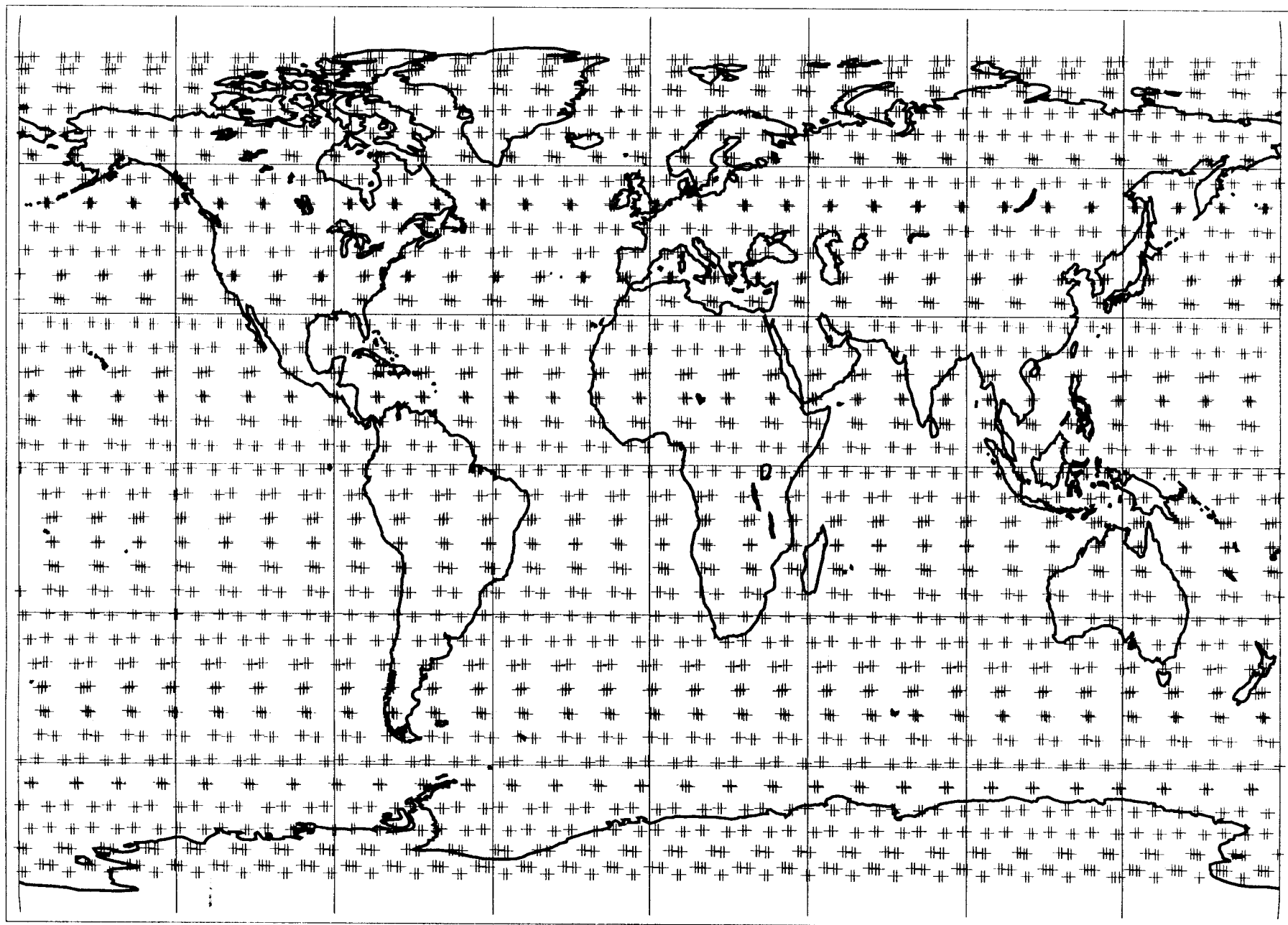


Fig 5





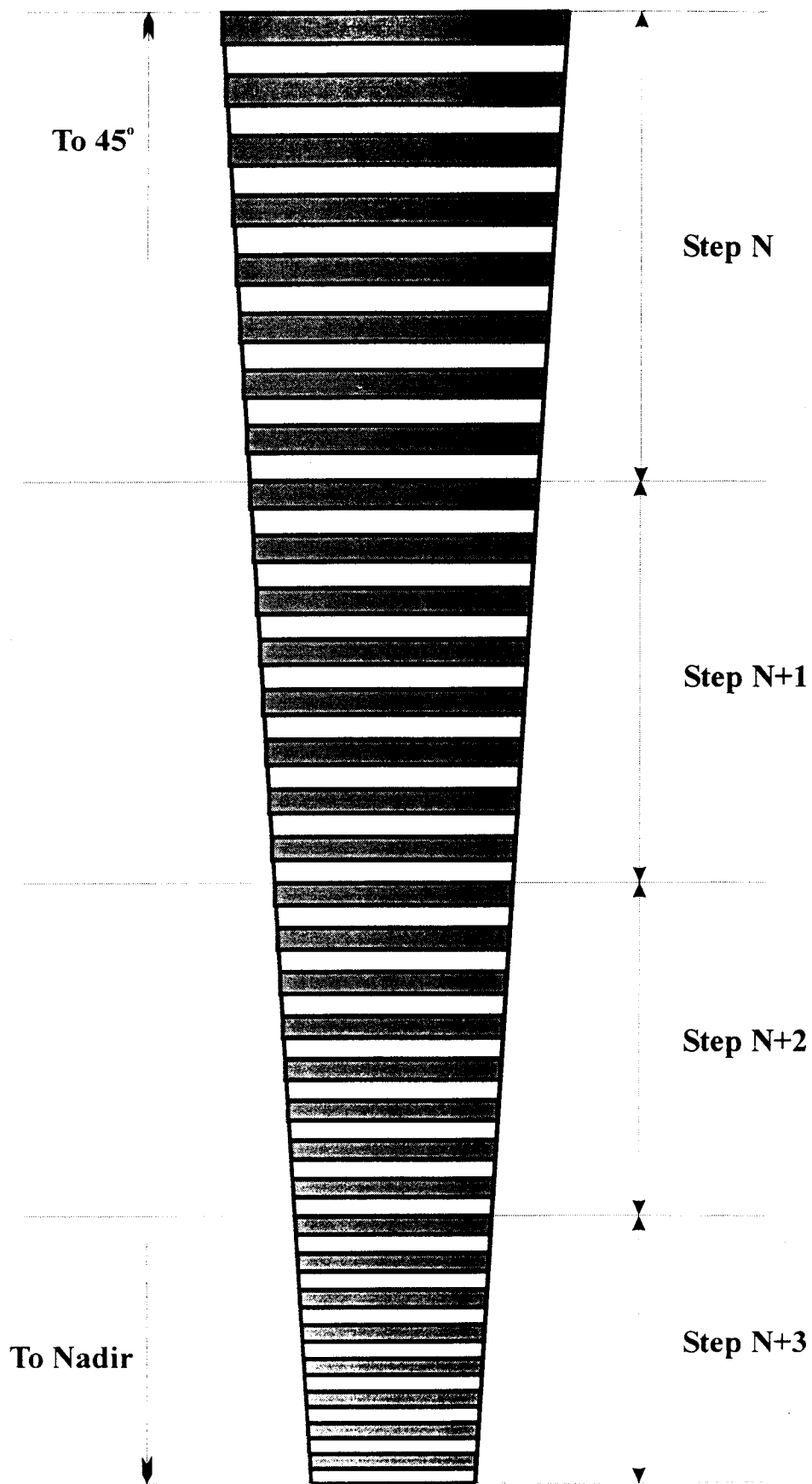


Fig. 8